JB
Journals.ASM.org

The Nla28S/Nla28 Two-Component Signal Transduction System Regulates Sporulation in *Myxococcus xanthus*

Zaara Sarwar and Anthony G. Garza

Department of Biology, Syracuse University, Syracuse, New York, USA

The response regulator Nla28 is a key component in a cascade of transcriptional activators that modulates expression of many important developmental genes in *Myxococcus xanthus*. In this study, we identified and characterized Nla28S, a histidine kinase that modulates the activity of this important regulator of *M. xanthus* developmental genes. We show that the putative cytoplasmic domain of Nla28S has the *in vitro* biochemical properties of a histidine kinase protein: it hydrolyzes ATP and undergoes an ATP-dependent autophosphorylation that is acid labile and base stable. We also show that the putative cytoplasmic domain of Nla28S transfers a phosphoryl group to Nla28 *in vitro*, that the phosphotransfer is specific, and that a substitution in the predicted site of Nla28 phosphorylation (aspartate 53) abolishes the phosphotransfer reaction. In phenotypic studies, we found that a mutation in *nla28S* produces a developmental phenotype similar to, but weaker than, that produced by a mutation in *nla28*; both mutations primarily affect sporulation. Together, these data indicate that Nla28S is the *in vivo* histidine kinase partner of Nla28 and that the primary function of the Nla28S/Nla28 two-component signal transduction system is to regulate sporulation genes. The results of genetic studies suggest that phosphorylation of Nla28S is important for the *in vivo* sporulation function of the Nla28S/Nla28 two-component system. In addition, the quorum signal known as A-signal is important for full developmental expression of the *nla28S-nla28* operon, suggesting that quorum signaling regulates the availability of the Nla28S/Nla28 signal transduction circuit in developing cells.

The rod-shaped Gram-negative soil bacterium *Myxococcus xanthus* is an ideal model for studying multicellular behavior in bacteria. In nature, *M. xanthus* is a microbial predator; large swarms of *M. xanthus* cells obtain nutrients from prey microbes by secreting pools of digestive enzymes (42). When they are starving, *M. xanthus* cells stop searching for prey. Instead, they build multicellular fruiting bodies that contain dormant, stress-resistant myxospores, which are well suited for survival during long bouts of starvation.

Fruiting-body development occurs in an ordered series of steps, starting with the starvation-induced accumulation of the intracellular alarmone guanosine-5′(tri)di-phosphate-3′diphosphate [(p)ppGpp] (10, 28, 44). Accumulation of (p)ppGpp informs individual cells that they are starving and that it is time to start the transition from feeding and growth to development. After (p)ppGpp accumulates, cells wait several hours before they begin to aggregate. During this period, referred to as preaggregation, cells ascertain whether the density of the starving cell population is sufficient to construct fruiting bodies. A diffusible quorum signal known as A-signal serves as the cell density indicator (21, 22, 33). If the level of this quorum signal is high enough, *M. xanthus* cells initiate the morphological changes needed to build fruiting bodies: cells move into aggregation centers, they form dome-shaped fruiting bodies, and they differentiate into myxospores. The execution of these morphological changes is controlled by progressively higher levels of a contact-stimulated, surface-associated cell-cell signaling protein known as C-signal (15, 16, 19, 26).

The behavioral and morphological events that occur during fruiting-body development are accompanied by large-scale changes in gene expression (5, 12, 17). *M. xanthus* developmental genes are activated sequentially, and in the case of several genes linked to sporulation, expression is spatially localized to the fruiting-body structure (13, 39). It is believed that developmental signals such as A-signal and C-signal coordinate these global changes in gene expression directly or indirectly through signal transduction circuits (18, 20). A number of transcriptional regulators that directly modulate expression of developmental genes have been identified (5, 25, 29, 30, 45). However, the signal transduction circuits that link particular developmental signals to the temporal and spatial expression of developmental genes remain largely undefined. Here, we define a signal transduction system (Nla28S/Nla28) that is expressed in response to A-signal accumulation and that regulates *M. xanthus* sporulation.

Nla28 was originally identified in a search for enhancer binding proteins (EBPs) that are important for fruiting-body development; a mutation in *nla28* causes a slight delay in aggregation and a strong decrease in the number of viable, stress-resistant myxospores (3). Recently, it was shown that Nla28 is a key component in an EBP cascade that regulates expression of important genes during early development (5). EBPs activate transcription of genes with σ^{54} promoter elements. The signal-activated ATPase function of EBPs allows σ^{54}-RNA polymerase to form an open σ^{54}-promoter complex and initiate transcription (34, 40, 49). EBPs typically activate gene expression in response to a specific interaction with a signal transduction partner that detects a particular environmental cue (46). Indeed, Nla28 is predicted to be a response regulator (RR) in a two-component signal transduction system (TCS) (6). In TCSs that contain EBPs such as Nla28, the

Received 15 February 2012 **Accepted** 25 June 2012

Published ahead of print 29 June 2012

Address correspondence to Anthony G. Garza, agarza@syr.edu.

Supplemental material for this article may be found at http://jb.asm.org/.

Copyright © 2012, American Society for Microbiology. All Rights Reserved.

doi:10.1128/JB.00225-12

TABLE 1 Bacterial strains and plasmids used in this study

Bacterial strain or plasmid	Relevant feature	Source or reference
Strains		
M. xanthus		
DK1622	Wild type	13a
DK4398	*asgB*	19a
AG1400	DK1622 Δ*nla28S*	This study
AG1401	Δ*nla28S* + *nla28S* (pZS202)	This study
AG1402	Δ*nla28S* + *nla28S* H242A (pZS210)	This study
E. coli		
TOP10	Cloning host	Invitrogen
BL21(DE3)	Expression host	Lab collection
NiCO21(DE3)	Expression host	New England Biolabs
Plasmids		
pCR-Blunt	Cloning vector, Kan^r	Invitrogen
pGEX-4T3	GST fusion expression vector, Amp^r	GE Healthcare
pET28b	His tag fusion expression vector, Kan^r	EMD Biosciences
pBJ114	Plasmid used for gene replacements and deletions, Kan^r *galK*$^+$	47
pZS93b	*nla28S* deletion cassette in pCR-Blunt	This study
pZS93	*nla28S* deletion cassette in pBJ114	This study
pZS108b	*nla28S*-cyt in pCR-Blunt	This study
pZS109b	*nla28* in pCR-Blunt	This study
pZS108	*nla28S*-cyt in pGEX-4T3	This study
pZS109	*nla28* in pGEX-4T3	This study
pZS134b	*envZ*-cyt in pCR-Blunt	This study
pZS135b	*ompR* in pCR-Blunt	This study
pZS134	*envZ*-cyt in pET28b	This study
pZS135	*ompR* in pET28b	This study
pZS187	*nla28S*-cyt H242A in pGEX-4T3	This study
pZS188	*nla28S*-cyt D386A in pGEX-4T3	This study
pZS191	*nla28*- D53A in pGEX-4T3	This study
pZS202	1,000-bp upstream region + *nla28S* in pCR-Blunt	This study
pZS210	1,000-bp upstream region + *nla28S* H242A in pCR-Blunt	

EBP activates gene expression in response to phosphorylation by a histidine kinase (HK) protein that detects a particular environmental signal (14). In the case of the *Escherichia coli* RR NtrC, which is one of the prototype EBPs, phosphorylation induces oligomerization and its ATPase activity, which is essential for transcriptional activation (1, 36, 49, 50).

The goals of this study were to identify and characterize the HK protein that modulates the activity of Nla28. Nla28S was classified as a strong candidate for the HK partner of Nla28 because DNA sequence analysis and expression studies suggest that the *nla28* and *nla28S* genes are part of the same operon (5, 6). Our *in vitro* studies showed that the purified putative cytoplasmic domain of Nla28S (GST-Nla28S-cyt) has the signature biochemical properties of an HK protein, that it is capable of transferring a phosphoryl group to purified Nla28 (GST-Nla28), and that the phosphotransfer between GST-Nla28S-cyt and GST-Nla28 is specific. In addition, we found that a mutation in *nla28S* produced a developmental phenotype similar to, but weaker than, that of a mutation in *nla28* (3); both mutations primarily affect sporulation. These results are consistent with our *in vitro* data indicating that Nla28S is the *in vivo* HK partner of Nla28, and they suggest that the primary developmental function of the Nla28S/Nla28 signal transduction circuit is to regulate sporulation.

MATERIALS AND METHODS

Strains and plasmids. The strains and plasmids used in this study are listed in Table 1, and the primers used in this study are listed in Table 2.

Media for growth and development. *M. xanthus* strains were grown at 32°C in CTTYE broth (1% Casitone, 0.2% yeast extract, 10 mM Tris [pH 8.0], 1 mM potassium phosphate [pH 7.6], 8 mM $MgSO_4$) or on plates containing CTTYE broth and 1.5% agar. CTTYE broth and CTTYE agar plates were supplemented with 50 μg/ml of kanamycin as needed. CTT soft agar contains 1.0% Casitone, 10.0 mM Tris-HCl (pH 8.0), 1.0 mM KH_2PO_4, 8.0 mM $MgSO_4$, and 0.7% agar. Fruiting-body development was carried out at 32°C on TPM agar plates (10 mM Tris [pH 7.6], 8 mM $MgSO_4$, 1 mM KH_2PO_4, 1.5% agar), on CF agar plates (10 mM Tris [pH 7.6], 0.015% Casitone, 8 mM $MgSO_4$, 1 mM KH_2PO_4, 2% sodium citrate, 1% sodium pyruvate, 1.5% agar), or in 6-well microtiter plates containing MC7 buffer (10 mM morpholinepropanesulfonic acid [MOPS; pH 7.0], 1 mM $CaCl_2$). *Escherichia coli* strains were grown in Luria-Bertani (LB) broth (1% tryptone, 0.5% yeast extract, 1% NaCl) or on plates containing LB broth and 1.5% agar. LB broth and LB agar plates were supplemented with 100 μg/ml of ampicillin or 50 μg/ml of kanamycin as needed. For protein expression and purification, *E. coli* strains were grown in 2XYT media (1.6% tryptone, 1% yeast extract, 0.5% NaCl) supplemented with 100 μg/ml of ampicillin or 50 μg/ml of kanamycin as needed.

Construction of the *nla28S* deletion mutant. The in-frame deletion of *nla28S* was generated using an adaptation (7) of the homologous recombination and counterselection method developed by Ueki et al. (47). The entire *nla28S* gene, except the last 4 bp that overlap the *nla28* gene, was deleted, yielding strain AG1400. The developmental expression pat-

TABLE 2 Primers used in this study

Primer use	Primer name (sequence[a])
In-frame deletion of *nla28S*	
nla28S upstream 700 bp	ZS92F (GGATGTCCGTGGGGAGAAACTCCGCAGTTGG)
	ZS92R (CGACGAGGATGCGGGCTGAGCGCCGTTCCTCTATCACGGGGCC)
nla28S downstream 700 bp	ZS93F (GGCCCCGTGATAGAGGAACGGCGCTCAGCCCGCATCCTCGTCGTG)
	ZS93R (CCGCTGGCCTCCTCGAAGACGCCTCGCCGC)
Cloning of *nla28S*, *nla28*, *envZ*, and *ompR*	
nla28S-cyt	ZS108F (GCGCCG*GGATCC*CGCGTCACCTCGCTGCTCAAG)
	ZS108R (GGGCGG*GAATTC*TCATGTTCCGACCTTGCGCATTTC)
nla28	ZS109F (GCGCCG*GGATCC*AGCTCAGCCCGCATCCTC)
	ZS109R (GGGCGG*GAATTC*TCACGACTCGGCCTCCGGGGCCTC)
envZ-cyt	ZS134F (GGCCGC*CATATG*GCGGATGACCGCACGCTGCTG)
	ZS134R (GCGCCG*AAGCTT*CCCTTCTTTTGTCGTGCCCTGC)
ompR	ZS135F (GGCCGC*CATATG*CAAGAGAACTACAAGATTCTGGTG)
	ZS135R (GCGCCG*AAGCTT*TGCTTTAGAGCCGTCCGGTAC)
Site-directed mutagenesis	
nla28S-cyt H242A	ZS188F (CCTTCACTCGGCGCGTGGCG**GCC**GACCTCATCTCCCCGCTGG)
	ZS188R (CCAGCGGGGAGATGAGGTC**GGC**CGCCACGCGCCGAGTGAAGG)
nla28S-cyt D386A	ZS189F (GGCCGTGCTGGAGGTCGTG**GCC**AACGGCATCGGCATGGCGC)
	ZS189R (GCGCCATGCCGATGCCGTT**GGC**CACGACCTCCAGCACGGCC)
nla28 D53A	ZS192F (CCTTTGACCTGGTCCTCACGGCCATGGCCATGCCCGAGCCGG)
	ZS192R (CCGGCTCGGGCATGGCCATGGCCGTGAGGACCAGGTCAAAGG)
qPCR	
nla28S (1,030 bp–1,209 bp of *nla28S*)	ZS155F (CAGTTGTTGCAGGTGAGTGC)
	ZS155R (GAAGGGCTGGAACAGTGAGG)
rpoD (519 bp–687 bp of *rpoD*)	ZS156F (CGCGGAAGAGAAGGAAGACG)
	ZS156R (CTTCTCACCATCCTCGATGC)

[a] Primer sequences are presented in the 5′ to 3′ direction. Restriction endonuclease recognition sites are presented in italics. Mutated codons are presented in bold type.

terns of *nla28*, which is located immediately downstream of *nla28S*, were similar in AG1400 and wild-type cells (data not shown), indicating that the in-frame deletion of *nla28S* does not alter *nla28* transcription via a polar effect.

***M. xanthus* development.** *M. xanthus* strains were grown to a density of ~5×10^8 cells/ml in CTTYE broth at 32°C with shaking. The cells were pelleted, the supernatant was removed, and the cells were resuspended to a density of 5×10^9 cells/ml in TPM buffer. Fifteen-microliter aliquots of the concentrated cell suspension were spotted onto TPM agar plates and CF agar plates and incubated in a humidity chamber at 32°C. For development in MC7 buffer-submerged cultures, a 200-μl aliquot of the concentrated cell suspension was added to each well of a 6-well plate and the cells were incubated in a 32°C humidity chamber. The progress of fruiting-body development was monitored visually 0, 12, 24, 48, 72, and 120 h after the aliquots were placed on TPM agar plates or CF agar plates using a Nikon Eclipse model E400 microscope. The images were captured using an Insight FireWire camera system and analyzed using SPOT, version 4.6, software (Diagnostic Instruments).

To determine the sporulation efficiency of *M. xanthus* strains, cells were allowed to develop for 120 h as described above, the cells were harvested, and the harvested cells were resuspended in 1 ml of TPM buffer. The resuspended cells were first dispersed by a 10-s burst of sonication using a model 100 Sonic Dismembrator (Fisher Scientific) that was set at an intensity of 1.5. Subsequently, the cells were subjected to three 10-s bursts of sonication using an intensity setting of 4, and the sonication-treated cells were incubated at 50°C for 2 h. The number of viable, heat- and sonication-resistant spores was determined by placing aliquots of the treated cells in warm CTT soft agar, pouring the CTT soft agar onto CTTYE agar plates, and counting the colonies that arose after 3 to 4 days of incubation at 32°C.

Protein expression and purification. PCR-generated DNA corresponding to the putative cytoplasmic domain of the *M. xanthus* Nla28S protein and the full-length *M. xanthus* Nla28 protein was cloned into the vector pGEX-4T3 (GE Healthcare) to create the N-terminal glutathione *S*-transferase (GST) fusion proteins GST-Nla28S-cyt and GST-Nla28, respectively (Fig. 1B). GST-Nla28S-cyt and GST-Nla28 were expressed in *E. coli* strain BL21(DE3). GST was expressed from the pGEX-4T3 plasmid (GE Healthcare) in *E. coli* strain BL21(DE3). PCR-generated DNA corresponding to the cytoplasmic domain of the *E. coli* EnvZ protein and the full-length *E. coli* OmpR protein were cloned into the vector pET28b (EMD Biosciences) to create N-terminal and C-terminal 6× histidine tags (His-EnvZ-cyt and His-OmpR, respectively). His-EnvZ-cyt and His-OmpR were expressed in *E. coli* strain NiCo21(DE3) (New England BioLabs). Cells were grown to an optical density at 600 nm (OD_{600}) of ~0.6 at 37°C with shaking at 210 rpm. Protein expression was induced by the addition of 0.1 mM isopropyl-β-D-thiogalactopyranoside (IPTG), and cell cultures were incubated for 12 h at 16°C with shaking at 210 rpm. Cells were harvested, resuspended in lysis buffer (100 mM sodium phosphate [pH 8.0], 300 mM NaCl, 10% glycerol, 1 mg/ml of lysozyme, 5 U/ml of DNase I, 1 μg/ml of pepstatin, 1 μg/ml of leupeptin), and lysed by three 30-s sonication bursts using a model 100 Sonic Dismembrator (Fisher Scientific) set at an intensity of 4. GST and the GST fusion proteins were purified using 5-ml GSTrapFF columns (GE Healthcare) on an AKTA purifier UPC 10 fast-performance liquid chromatography (FPLC) system (GE). GST fusion proteins were eluted from the GSTrapFF columns using GST elution buffer (100 mM Tris [pH 7.4], 300 mM NaCl, 1 mM reduced glutathione). The His-tagged proteins were purified using 5-ml HisPur Cobalt columns (Thermo Scientific) on an AKTA purifier UPC 10 FPLC system (GE Healthcare). The His-tagged proteins were eluted from the HisPur Cobalt columns using a step elution method with elution buffer (100 mM Tris [pH 7.4], 300 mM NaCl) containing 20 mM, 100 mM, 250 mM, and 500 mM imidazole. All purified proteins were concentrated using Amicon Ultra centrifugal filter units (Millipore). Protein expression and purification were monitored visually using sodium dodecyl sulfate-

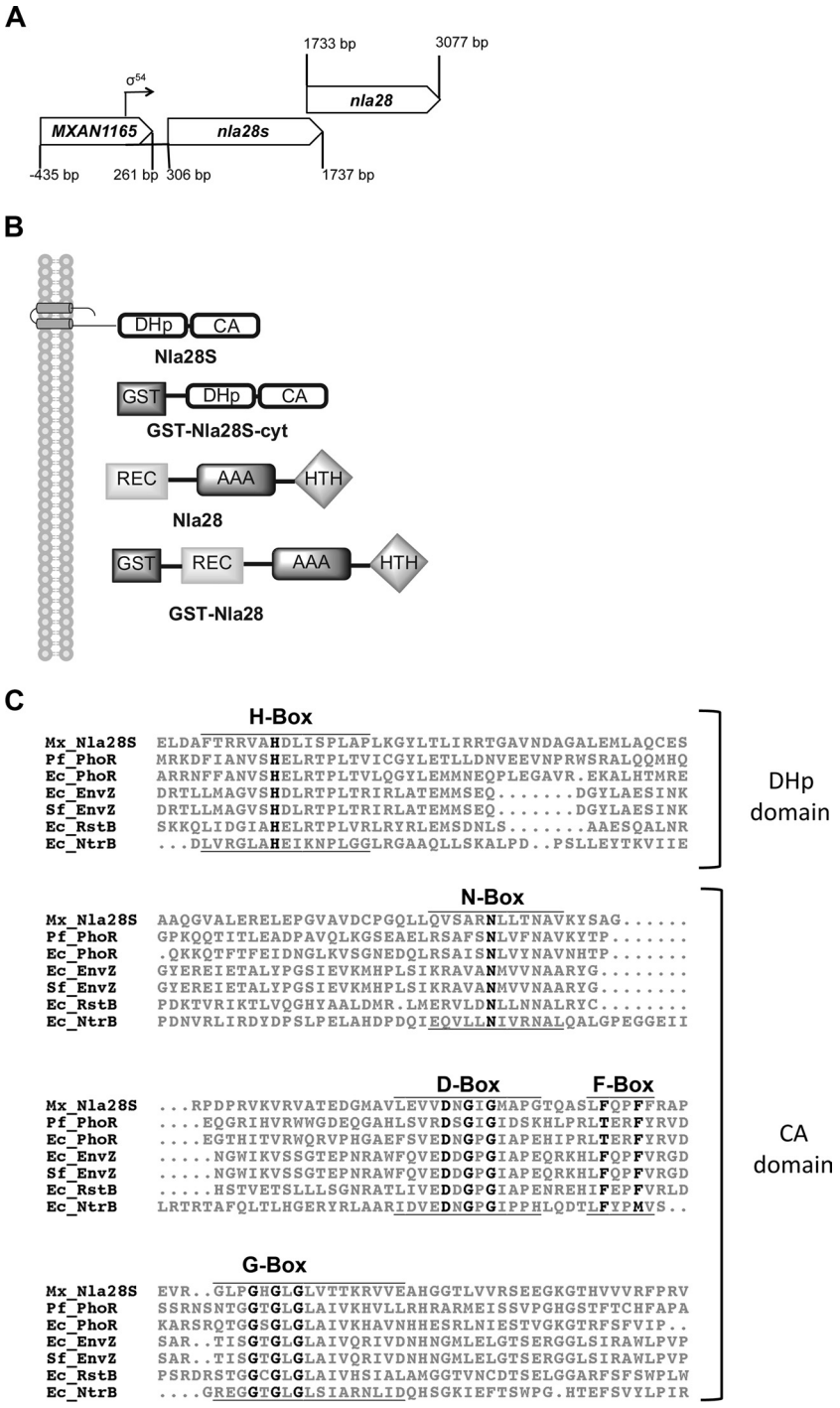

FIG 1 Organization of the *nla28S-nla28* operon, domain organization of relevant proteins, and an Nla28S sequence alignment. (A) Organization of the *nla28S-nla28* operon. (B) Domain organization of Nla28S (476 amino acids), GST-Nla28S-cyt (an N-terminal GST fusion to the C-terminal 270 amino acids of Nla28S), Nla28 (447 amino acids), and GST-Nla28 (an N-terminal GST fusion to full-length Nla28). (C) Alignment of the Nla28S amino acid sequence with those of other well-characterized HKs indicates that Nla28S has all of the conserved HK sequence motifs. The alignment was generated using ClustalW2. The H-, N-, D-, F-, and G-boxes are shown, and the conserved residues are in black and bold type. HKs from *Escherichia coli* (Ec), *Pseudomonas fluorescens* (Pf), *Shigella flexneri* (Sf), and *Myxococcus xanthus* (Mx) are shown. GST, glutathione *S*-transferase; DHp, dimerization and histidine phosphorylation domain; CA, catalytic and ATPase domain; REC, receiver domain; AAA, ATPase domain; HTH, helix-turn-helix domain.

polyacrylamide gel electrophoresis (SDS-PAGE). The concentration of purified protein was determined using Bradford assays. Circular-dichroism (CD) spectroscopy was used to monitor the folding of the purified proteins. CD spectra were collected on a model 202 spectropolarimeter (Aviv Biomedical). CD data were recorded from 195 nm to 260 nm at 10°C in a 1-mm-path-length cell. The spectral bandwidth was 1.0 nm, the step size was 1 nm, and the averaging time was 10 s. Each spectrum was recorded in triplicate.

ATP hydrolysis assay. The ATP-hydrolyzing activity of purified GST-Nla28S-cyt was investigated using a standard colorimetric assay that couples the hydrolysis of ATP with the oxidation of NADH (23). In this assay, the change in absorbance at 340 nm caused by the oxidation of NADH to NAD is used to monitor the amount of ATP hydrolyzed to ADP. Briefly, 5 μM purified GST-Nla28S-cyt in ATPase buffer (50 mM Tris [pH 7.4], 5 mM $MgCl_2$, 75 mM KCl) was incubated with 1 U of L-lactate dehydrogenase (Roche), 1 U of pyruvate kinase (Roche), 0.5 mM phosphoenolpyruvate, 0.3 mM NADH, and different concentrations of ATP (0.1 mM, 0.3 mM, or 2 mM) at room temperature. Absorbance readings at 340 nm were taken using a Spectronic GENESYS 6 UV-visible spectrophotometer (Thermo Scientific) every 30 s for a total of 5 min to measure the oxidation of NADH to NAD, which is proportional to the conversion of ATP to ADP. His-EnvZ-cyt was used as a positive control and purified GST was used as a negative control for the ATPase assay.

Autophosphorylation assay. A 5 μM aliquot of purified GST-Nla28S-cyt was incubated with 500 μM ATP and 30 μCi of [γ-^{32}P]ATP in kinase buffer (5 mM $MgCl_2$, 2 mM dithiothreitol [DTT], 100 mM Tris [pH 7.4]) at room temperature. At 0, 0.5, 1, 5, 10, 30, and 60 min after the reaction was started, 10-μl aliquots of the reaction mixture were removed and the reaction was stopped by the addition of 6× SDS-PAGE loading buffer (375 mM Tris-HCl [pH 6.8], 9% SDS, 50% glycerol, 9% β-mercaptoethanol, 0.03% bromophenol blue). Excess [γ-^{32}P]ATP was removed from the samples using Zeba Micro Spin desalting columns (Pierce Protein Research Products, Thermo Scientific). His-EnvZ-cyt was used as a positive control and purified GST was used as a negative control for the autophosphorylation assay. The samples were separated using SDS-PAGE and visualized using a Typhoon 9410 variable-mode imager (GE Healthcare).

To determine the acid and base stability of phosphorylated GST-Nla28S-cyt, a 60-min autophosphorylation reaction was performed as described above. The reaction was stopped by the addition of 6× SDS-PAGE loading buffer, and then the sample was treated with 0.1 M HCl or 1 M NaOH for 20 min. The samples were separated using SDS-PAGE and visualized using a Typhoon 9410 variable-mode imager (GE Healthcare).

Phosphotransfer assay. Purified GST-Nla28S-cyt was allowed to autophosphorylate for 60 min as described above, and excess [γ-^{32}P]ATP was removed from the reaction mixture using Zeba Micro Spin desalting columns (Pierce Protein Research Products, Thermo Scientific). Subsequently, 10 μl of kinase buffer containing 5 μM phosphorylated GST-Nla28S-cyt and 5 μM purified GST-Nla28 was incubated at room temperature. Samples were removed from the reaction mixture at 0, 0.25, 0.5, 1, 5, 10, 30, and 60 min after the reaction was started, and the reaction was stopped by the addition of 6× SDS-PAGE loading buffer. The samples were separated using SDS-PAGE, and the phosphotransfer from GST-Nla28S-cyt to GST-Nla28 was visualized using a Typhoon 9410 variable-mode imager (GE Healthcare). The phosphotransfer from His-EnvZ-cyt to its cognate response regulator His-OmpR was used as a positive control for the above-described assay. As a negative control for the phosphotransfer assay, a reaction mixture containing phosphorylated GST-Nla28S-cyt was incubated with an equimolar amount of GST. In order to investigate the specificity of phosphotransfer from Nla28S to Nla28, phosphotransfer reactions between GST-Nla28S-cyt and His-OmpR and between His-EnvZ-cyt and GST-Nla28 were carried out and analyzed as described above.

Phosphorylation of response regulators by [^{32}P]acetyl phosphate. [^{32}P]acetyl phosphate was synthesized as described by Quon et al. (37) and added to kinase buffer containing 5 μM GST-Nla28, and the reaction mixture was incubated at room temperature for 30 min. The reaction was terminated by addition of 6× SDS-PAGE loading buffer. Excess [^{32}P]acetyl phosphate was removed using Zeba Micro Spin desalting columns (Thermo Scientific). The phosphorylation of GST-Nla28 was analyzed by SDS-PAGE and phosphorimaging as described above. His-OmpR was used as a positive control and purified GST was used as a negative control for the acetyl phosphate phosphorylation assay.

Expression analysis of *nla28S*. To determine the expression profile of the *nla28S* gene during early development, DK1622 was allowed to develop in MC7 buffer-submerged cultures as described above and samples were taken at 0, 0.5, 1, 1.5, 2, 2.5, 3, and 4 h poststarvation for RNA isolation. To examine *nla28S* expression in an *asg* mutant background, wild-type and *asgB* cells were allowed to develop in MC7 buffer-submerged culture as described above and samples were removed for RNA isolation at the peak expression time point (2 h poststarvation) of *nla28S* in wild-type cells. The procedure was repeated 3 times for each strain.

Total RNA was isolated using the RNAprotect Bacteria Reagent (Qiagen) and RNeasy Plus Minikit (Qiagen) according to the manufacturer's protocol. The iScript cDNA synthesis kit (Bio-Rad) was used to generate cDNA from the purified RNA samples. A 10-fold dilution series of the pooled cDNA from the three replicate RNA samples from wild-type or *asgB* cells was used for the quantitative PCR (qPCR) experiments. The qPCR experiments were also performed in triplicate. The expression of *nla28S* in wild-type or *asgB* cells was normalized to that of *rpoD*, which is expressed at similar levels during growth and development (see Fig. S1 in the supplemental material). Primers for qPCR were designed to produce 180-bp to 200-bp amplicons of the *nla28S* and *rpoD* genes. The qPCR mixtures contained 300 mM each primer, 10 μl of the 2× iQ SYBR green Supermix (Bio-Rad), 5 μl of diluted cDNA, and nuclease-free water to a total volume of 20 μl. qPCR was performed on the iCycler iQ system (Bio-Rad) with the following conditions: 1 cycle of 95°C for 2 min and 40 cycles of 95°C for 15 s, 55°C for 30 s, and 72°C for 30 s. Standard-curve R^2 values and amplification efficiency values ranged from 0.990 to 1.0 and 90.0% to >100%, respectively. The amplification efficiency was calculated using the program LinRegPC (38).

RESULTS

Identification of a potential HK partner for Nla28. The putative HK gene *nla28S* (MXAN1166) is located directly upstream of *nla28* (MXAN1167) (6), and the two genes show similar expression patterns during development (5), suggesting that *nla28S* and *nla28* are likely to be part of the same operon (Fig. 1A). Since HK and RR genes that code for TCS partners are often located in the same operon (11), Nla28S was considered a prime candidate for the *in vivo* HK partner of Nla28. Nla28S has similarity to type I histidine kinase proteins such as PhoR and EnvZ, which have N-terminal domains for binding extracellular signal molecules, membrane-spanning regions, and C-terminal cytoplasmic kinase domains (14). An alignment of the conserved regions in the C termini of known HK proteins and the corresponding regions in the C terminus of Nla28S is shown in Fig. 1C.

Nla28S has the *in vitro* properties of an HK protein. When they detect a specific signal, HKs bind and hydrolyze ATP and autophosphorylate at a conserved histidine residue (14). To confirm that Nla28S was indeed a functional HK protein, we first examined the *in vitro* ATPase activity of purified GST-Nla28S-cyt using a colorimetric assay that couples ATP hydrolysis to NADH oxidation (23). As shown in Fig. 2, GST-Nla28S-cyt hydrolyzed ATP and the amount of hydrolyzed ATP increased linearly with time. Next, we examined the *in vitro* autophosphorylation activity of purified GST-Nla28S-cyt. When it was incubated with [γ-^{32}P]ATP, GST-Nla28S-cyt autophosphorylated within 30 s and the level of GST-Nla28S-cyt autophosphorylation increased at every time point up to 60 min (Fig. 3A). Phosphorylated histidine residues are acid labile but base stable (32). To examine whether phosphorylated GST-Nla28S-cyt has such properties, purified GST-Nla28S-cyt was incubated with [γ-^{32}P]ATP for 60 min, and the samples were treated with acid or base for 20 min or left untreated for 20 min. Figure 3B shows that in the sample treated with

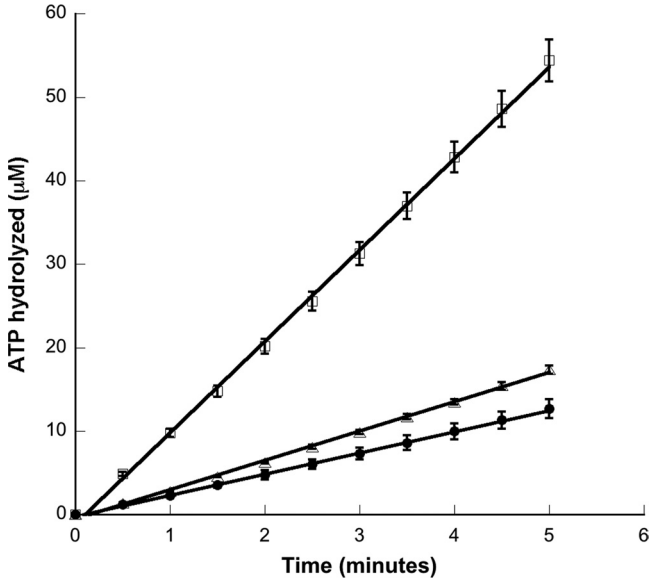

FIG 2 ATP hydrolysis activity of GST-Nla28S. A standard colorimetric assay that couples the hydrolysis of ATP to the oxidation of NADH was used to determine ATP hydrolysis activity of GST-Nla28S-cyt. The plot shows the concentration of ATP hydrolyzed by GST-Nla28S-cyt versus the time of the reaction. The initial ATP concentrations in the reactions were 0.1 mM (filled circles), 0.3 mM (open triangles), and 2 mM (open squares). Each measurement was done in triplicate. Error bars represent standard errors of the means of three replicates.

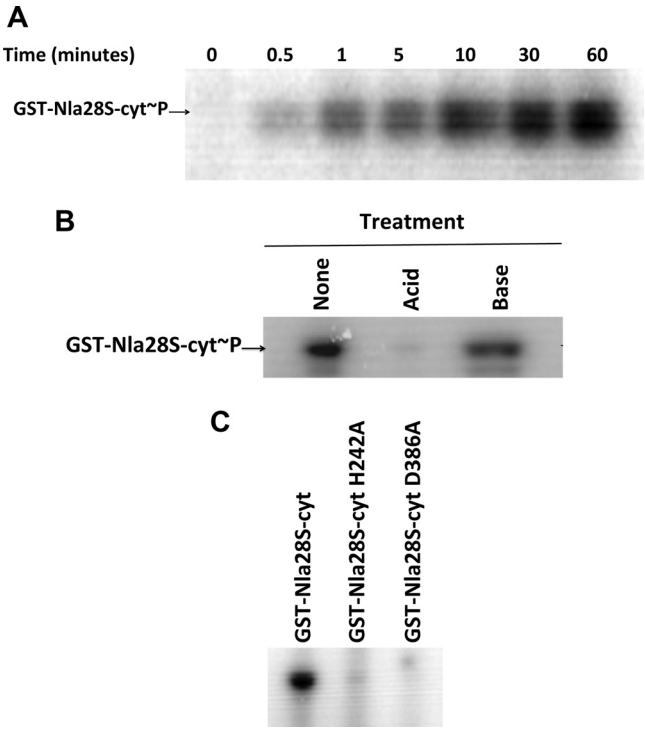

FIG 3 *In vitro* autophosphorylation activity of GST-Nla28S-cyt. (A) Time course of the autophosphorylation activity of GST-Nla28S-cyt (GST-Nla28S-cyt~P) incubated with [γ-^{32}P]ATP at room temperature. (B) Autophosphorylation activity of GST-Nla28S-cyt incubated with [γ-^{32}P]ATP for 60 min and treated with 0.1 N HCl or 1 N NaOH for 20 min at room temperature. (C) Autophosphorylation activity of GST-Nla28S-cyt, GST-Nla28S-cyt H242A, and GSTNla28S-cyt D386A incubated with [γ-^{32}P]ATP for 60 min at room temperature.

base, the level of GST-Nla28S-cyt phosphorylation is similar to that in the untreated sample, but little or no phosphorylated GST-Nla28S-cyt was detected after acid treatment. In additional experiments, we examined the kinetics of Nla28S autophosphorylation by performing ATPase assays with different concentrations of ATP. The calculated K_m of 0.518 mM and k_{cat} of 0.65 min^{-1} are comparable to the kinetic parameters of other characterized HKs such as CheA from *E. coli* (0.77 mM and 3 min^{-1}), CheA from *Sinorhizobium melliloti* (0.1 mM and 0.48 min^{-1}), and CheA$_1$ and CheA$_2$ from *Rhodobacter sphaeroides* (0.25 mM and 0.36 min^{-1} and 0.61 mM and 0.78 min^{-1}, respectively) (35). Thus, the results of all our *in vitro* biochemical assays support the idea that Nla28S is an HK protein.

His242 in the H-box of Nla28S is crucial for *in vitro* autophosphorylation. The transmitter domain of HKs is divided into the dimerization and histidine phosphorylation domain (DHp) and the catalytic and ATP binding domain (CA). The conserved His residue of HKs that is autophosphorylated is located within the H-box in the DHp domain. Sequence analysis of Nla28S revealed that His242 in the H-box (Fig. 1C) is the putative site of autophosphorylation in Nla28S. To test this finding, we examined the autophosphorylation of the GST-Nla28S-cyt H242A mutant. Figure 3C shows that after 60 min of incubation with [γ-^{32}P]ATP, the level of autophosphorylation of GST-Nla28S-cyt H242A was less than 1% that of GST-Nla28S-cyt. This result suggests that His242 is the likely site of Nla28S autophosphorylation.

The putative CA domain of Nla28S is required for *in vitro* autophosphorylation. The CA domain consists of the four conserved sequence motifs (N-, D-, F-, and G-boxes) that form a pocket for the binding and hydrolysis of ATP (4). The conserved D-box Asp in the CA domain of HK proteins plays an important role in ATP binding by directly interacting with ATP via a hydrogen bond with the N6-amine of the adenine moiety (4). In Nla28S, residue 386 is the putative D-box Asp (Fig. 1C). To examine the importance of the Nla28S CA domain in autophosphorylation, we generated the D386A substitution in GST-Nla28S-cyt (GST-Nla28S-cyt D386A). After incubation with [γ-^{32}P]ATP for 60 min, the level of phosphorylation of GST-Nla28S-cyt D386A was less than 1% that of GST-Nla28S-cyt (Fig. 3C). This finding indicates that the putative D-box Asp and, presumably, the CA domain of Nla28S are important for *in vitro* autophosphorylation.

Nla28 uses acetyl phosphate as an *in vitro* phosphodonor. The receiver domain of RRs catalyzes the phosphotransfer from HK proteins (2). In addition, many RRs can catalyze a phosphotransfer from small molecule donors such as acetyl phosphate (27). Nla28 is known to bind to the σ^{54} promoters of several developmental genes and to be important for expression of these genes in developing cells (5; K. Murphy, T. Li, and A. Garza, personal communication), which is consistent with its proposed function as a transcriptional activator. To investigate whether Nla28 has the *in vitro* properties of an RR, purified GST-Nla28 was incubated with [^{32}P]acetyl phosphate for 30 min. Figure 4A shows that phosphorylated GST-Nla28 was detected when incubated with [^{32}P]acetyl phosphate but not with [γ-^{32}P]ATP (negative control). This finding indicates that GST-Nla28 is capable of catalyzing a phosphotransfer reaction *in vitro*, which is a signature property of bacterial RRs.

Nla28S transfers its phosphoryl group to Nla28 *in vitro*. To examine whether Nla28S and Nla28 can serve as *in vitro* phospho-

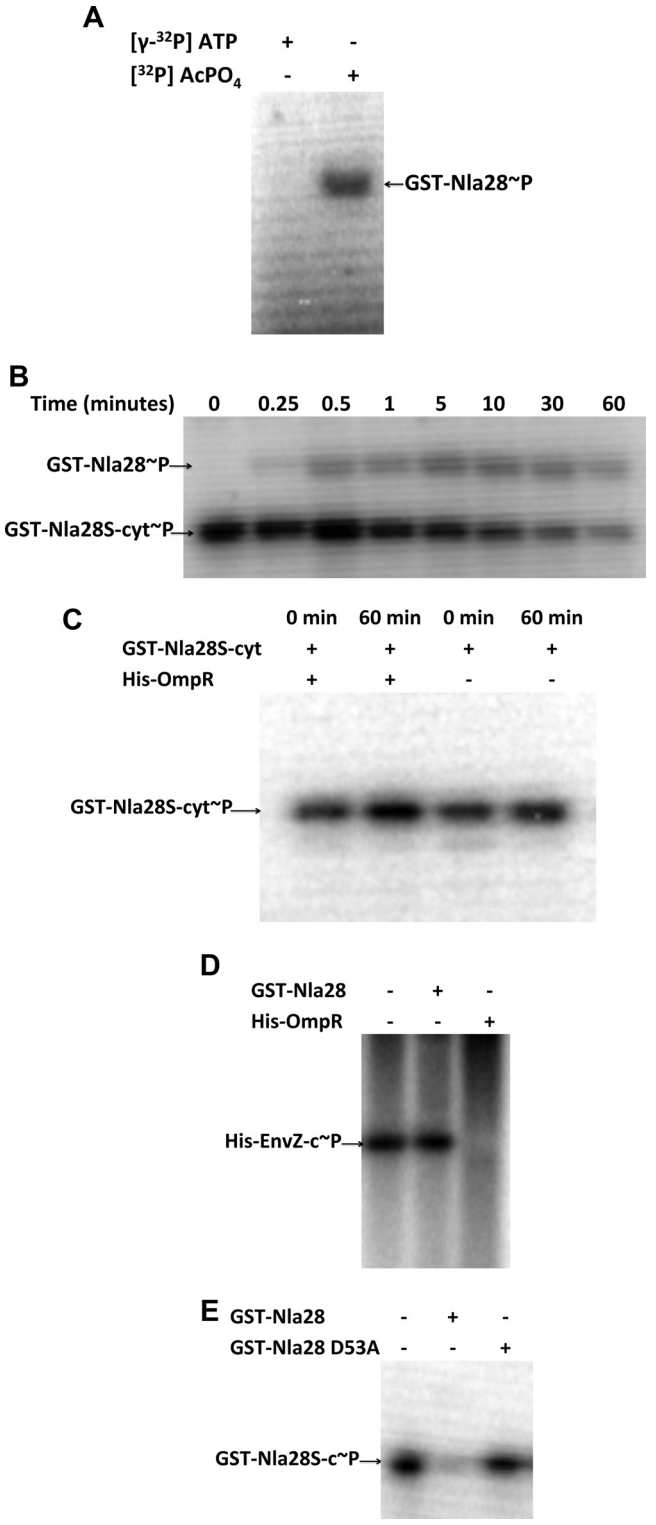

FIG 4 *In vitro* phosphotransfer assays. (A) GST-Nla28 was incubated with [γ-^{32}P]ATP or [^{32}P]acetyl phosphate ([^{32}P]$AcPO_4$) for 30 min. (B) Autophosphorylated GST-Nla28S-cyt (GST-Nla28S-cyt~^{32}P) was incubated with GST-Nla28 at room temperature. (C) Autophosphorylated GST-Nla28S-cyt was incubated with His-OmpR or in kinase buffer alone at room temperature for 60 min. (D) Autophosphorylated His-EnvZ-cyt was incubated in kinase buffer alone, with GST-Nla28, or with His-OmpR at room temperature for 60 min. (E) Autophosphorylated GST-Nla28S-cyt was incubated in kinase buffer alone, with GST-Nla28, or with GST-Nla28 D53A at room temperature for 60 min.

transfer partners, which would be consistent with the idea that they form an *in vivo* TCS, purified GST-Nla28S-cyt was incubated with [γ-^{32}P]ATP for 60 min, the [γ-^{32}P]ATP was removed, and then the phosphorylated GST-Nla28S-cyt was incubated with an equimolar amount of purified GST-Nla28 for various amounts of time before the reaction was terminated (Fig. 4B). An HK-to-RR phosphotransfer is detected by the appearance of a second band corresponding to the radiolabeled RR or by the depletion of radiolabel from the HK, which indicates that the HK-to-RR phosphotransfer was followed by RR dephosphorylation (24). As shown in Fig. 4B, phosphorylation of GST-Nla28 was detected after only 15 s of incubation with GST-Nla28S-cyt. The level of GST-Nla28 phosphorylation increased after an additional 15 s of incubation with GST-Nla28S-cyt and remained fairly steady with longer incubation periods up to 60 min, when the level of phosphorylated GST-Nla28 decreased. Over the same time course of incubation, the general trend for GST-Nla28S-cyt was a decrease in phosphorylation (Fig. 4B). In contrast, the level of phosphorylated GST-Nla28S-cyt remained relatively constant over time when it was incubated with His-OmpR, which is a polyhistidine-tagged version of the noncognate *E. coli* RR OmpR (Fig. 4C). Moreover, no band corresponding to phosphorylated His-OmpR was observed, even after 60 min of incubation with phosphorylated GST-Nla28S-cyt (Fig. 4C). In addition, after 60 min of incubation with phosphorylated His-EnvZ-cyt (Fig. 4D), which is a polyhistidine-tagged version of the noncognate *E. coli* HK EnvZ, no phosphorylated GST-Nla28 was detected. Furthermore, GST-Nla28 did not cause His-EnvZ-cyt radiolabel to become depleted after 60 min of incubation (Fig. 4D). In contrast, after phosphorylated His-EnvZ-cyt and His-OmpR (EnvZ and OmpR are TCS partners in *E. coli*) were incubated for 60 min, the radiolabel from His-EnvZ-cyt was depleted (Fig. 4D). Presumably, His-EnvZ-cyt successfully transferred a phosphoryl group to His-OmpR and His-OmpR was subsequently dephosphorylated. Taken together, these findings indicate that Nla28S and Nla28 are *in vitro* phosphotransfer partners and that the Nla28S-to-Nla28 phosphotransfer is specific, suggesting that Nla28S is likely to be the *in vivo* HK partner of Nla28.

The Asp53 residue of Nla28 is required for *in vitro* phosphotransfer. The HK-to-RR phosphotransfer reaction is catalyzed by the receiver domain of the RR, which contains a conserved phosphor-accepting Asp residue. To investigate whether the conserved Asp53 residue in Nla28 is important for its phosphorylation, we generated a D53A substitution in GST-Nla28 (GST-Nla28 D53A) and performed phosphotransfer assays with purified GST-Nla28S-cyt and GST-Nla28 D53A (Fig. 4E). After 60 min of incubation with phosphorylated GST-Nla28S-cyt, no band corresponding to the phosphorylated GST-Nla28 D53A was detected. Furthermore, there was negligible depletion of radiolabel from the phosphorylated GST-Nla28S-cyt. These results indicate that Nla28 requires a conserved Asp residue for phosphotransfer from a cognate HK.

An *nla28S* mutation primarily affects sporulation. If Nla28S and Nla28 are partners in the same TCS, then a mutation in *nla28S* is likely to produce developmental defects that are similar to those produced by an *nla28* mutation. A mutation in the *nla28* gene causes a slight aggregation delay but a strong (>10-fold) decrease in sporulation efficiency relative to that of wild-type cells (3). To examine whether a mutation in *nla28S* produces similar developmental defects, we constructed a strain of *M. xanthus* that contains an in-frame deletion of *nla28S* (see Materials and Methods).

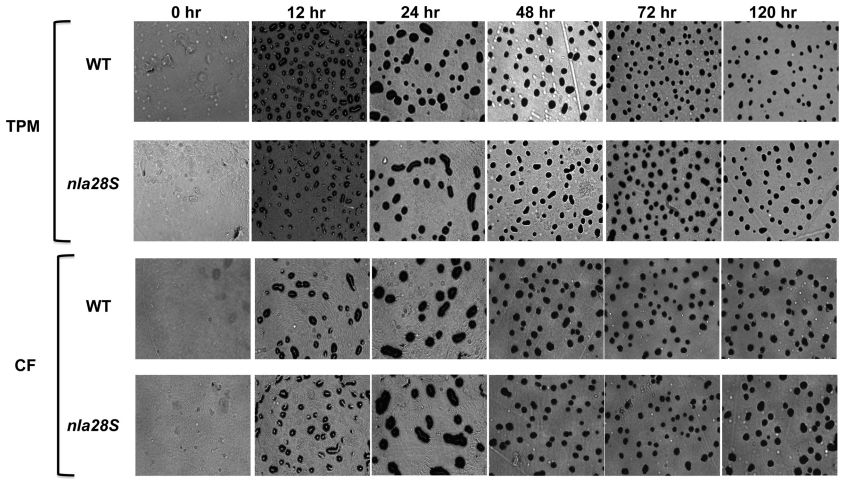

FIG 5 Development phenotypes of wild-type (WT) and Δ*nla28S* mutant cells. Wild-type and Δ*nla28S* cells were spotted onto TPM agar plates (top two panels) or CF agar plates (bottom two panels), and the progress of fruiting-body development was monitored for 5 days using a Nikon Eclipse model E400 microscope at a total magnification of ×40. Photographs were taken at 0, 24, 48, 72, and 120 h poststarvation.

When we placed Δ*nla28S* and wild-type cells on TPM starvation agar plates, no differences in aggregation or fruiting-body formation were observed (Fig. 5). However, Δ*nla28S* cells did show a slight (about 1.5-fold) decrease in sporulation efficiency relative to that of wild-type cells (Table 3). When we monitored the development of Δ*nla28S* and wild-type cells on CF agar, which induces a more gradual starvation than TPM agar, we found that aggregation and fruiting-body formation proceeded similarly. The sporulation efficiency of Δ*nla28S* cells was, however, reduced about 4-fold relative to that of wild-type cells (Table 3). These results indicate that the Δ*nla28S* mutation affects sporulation but not aggregation. Thus, it seems that the primary function of Nla28S and Nla28 is to regulate sporulation, which supports our proposal that Nla28S and Nla28 are *in vivo* TCS partners. A potential explanation for the finding that the Δ*nla28S* mutation produces a much weaker sporulation defect than the *nla28* mutation is mentioned in the Discussion.

To examine whether Nla28S phosphorylation is important for the *in vivo* sporulation function of the Nla28S/Nla28 TCS, two *nla28S* alleles were introduced into the native *nla28S* locus in the Δ*nla28S* mutant and placed under the transcriptional control of the native *nla28S-nla28* operon promoter (5). One of the *nla28S* alleles encodes wild-type Nla28S, and the other allele encodes Nla28S H242A, an altered version of Nla28S that is defective for *in vitro* autophosphorylation (Fig. 3C). The *nla28S* allele encoding the wild-type Nla28S protein rescued the sporulation defect of the Δ*nla28S* mutant (96.7% ± 6.77% of wild-type sporulation efficiency), whereas the *nla28S* allele encoding the altered Nla28S protein failed to rescue the sporulation defect of the Δ*nla28S* mutant (26.2% ± 2.14% of wild-type sporulation efficiency). These findings suggest that the *in vivo* phosphorylation of Nla28S is indeed important for the sporulation function of the Nla28S/Nla28 two-component system.

TABLE 3 Sporulation efficiency of wild-type and Δ*nla28S* mutant cells

Medium	% sporulation efficiency (mean ± SD)[a]			
	Wild type (DK1622)	Δ*nla28S* (AG1400)	Δ*nla28S* + *nla28S* (AG1401)	Δ*nla28S* + *nla28S* H242A (AG1402)
TPM	100 ± 9.72	65.4 ± 7.13		
CF	100 ± 5.15	22.6 ± 1.61	96.7 ± 6.77	26.2 ± 2.14

[a] All spore assays were performed in triplicate. The mean sporulation efficiencies of AG1400, AG1401, and AG1402 mutant cells are shown as percentages of that of DK1622 (wild-type) cells.

Developmental expression of *nla28S* is A-signal dependent. As shown in Fig. 6A, we monitored the developmental expression pattern of *nla28S* using qPCR. As previously reported (5), the developmental expression pattern of *nla28S* is similar to that of *nla28*: *nla28S* mRNA levels start to increase at 1 h poststarvation (which is early in preaggregation), they peak at 2 h poststarvation, and they return to vegetative levels between 2 and 3 h poststarvation. Since A-signal production is activated about 1 to 2 h poststarvation (13b, 20), we speculated that developmental expression of *nla28S* might be A-signal dependent. To test this proposal, we examined the levels of *nla28S* mRNA in *asgB* cells, which are defective for A-signal production (20), and wild-type cells at 2 h poststarvation. As shown in Fig. 6B, expression of *nla28S* mRNA was reduced about 2-fold in *asgB* cells relative to that of wild-type cells. To confirm that expression of *nla28S* is A-signal dependent, *asgB* cells were allowed to develop in MC7 buffer that was previously conditioned with exogenous A-signal by wild-type cells. When exogenous A-signal was provided to *asgB* cells, expression of *nla28S* mRNA was completely restored (Fig. 6B). These findings indicate that full expression of *nla28S* and, presumably, *nla28* in developing cells requires A-signal; expression of the genes for the Nla28S/Nla28 TCS components is modulated by A-signal.

DISCUSSION

The assembly of multicellular structures such as *M. xanthus* fruiting bodies depends on signal transduction networks that tie extracellular and intracellular signals to stage-specific changes in gene expression. *M. xanthus* has a plethora of signal transduction genes that can fulfill this need to link developmental signals to changes in gene expression (6). This includes 272 TCS genes, which constitute about 3.7% of the *M. xanthus* genome (6). Many of these TCS genes are differentially expressed during fruiting-body development (5) (Gene Expression Omnibus [GEO] accession number

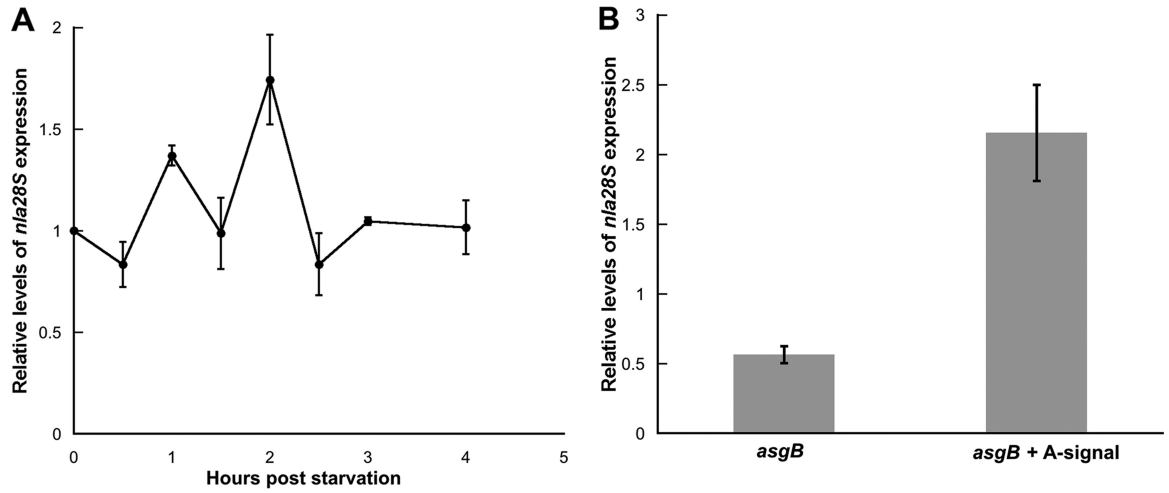

FIG 6 Expression of *nla28S* in wild-type and *asgB* mutant cells. (A) qPCR was used to examine developmental expression of *nla28S* in wild-type (DK1622) cells. The *nla28S* expression levels shown are relative to the levels found in growing wild-type cells (0 h). The values are means derived from three replicates. The error bars indicate standard deviations of the means. (B) qPCR was used to examine developmental expression of *nla28S* in *asgB* mutant (DK4398) cells at the time of its peak expression (2 h poststarvation) in wild-type cells. The *nla28S* expression levels shown are relative to the levels found in wild-type cells at 2 h poststarvation. The values are means derived from three replicates. The error bars are standard errors of the means.

GSE13523), and 35 TCS genes that are important for the developmental process have been identified (41). However, much of the work on TCS components has concentrated on RRs and their target developmental genes (3, 5, 8, 9, 48; Murphy et al., personal communication); few of the HK and RR signal transduction circuits that modulate developmental gene expression have been defined, and very little is known about the signals that activate the characterized HK and RR circuits.

In this study, we identified and characterized the HK partner of Nla28, a member of the EBP family of RRs (6). A mutation in the *nla28* gene causes a slight aggregation delay but a strong (>10-fold) decrease in sporulation efficiency relative to that of wild-type cells (3), suggesting that the primary targets of Nla28-mediated transcription are sporulation genes. Indeed, most of the developmental genes that are known to be directly regulated by Nla28, including *nla6* and *actB*, are primarily involved in sporulation (3, 5, 7; Murphy et al., personal communication). Nla28S was identified as a potential HK partner of the Nla28 RR based on data suggesting that *nla28S* and *nla28* are part of the same developmentally regulated operon (5, 6). The *in vitro* studies presented here indicate that Nla28S is a functional HK protein, it is capable of transferring a phosphoryl group to Nla28, and the phosphotransfer between the two proteins is specific (Fig. 1 to 4). Thus, all the *in vitro* experiments that we performed in this study support the idea that Nla28S and Nla28 are partners in a TCS and, based on studies of Nla28 (3, 5; Murphy et al., personal communication), the primary output of this TCS is transcription of sporulation genes.

Since our *in vitro* work indicated that Nla28S and Nla28 are part of the same TCS and Nla28 appears to be a regulator of sporulation genes (3, 5; Murphy et al., personal communication), we predicted that an *nla28S* mutation would primarily affect sporulation. Under the stringent starvation conditions of TPM agar and the gradual starvation conditions of CF agar, the Δ*nla28S* mutant showed no obvious aggregation defect (Fig. 5). However, the sporulation efficiency of the Δ*nla28S* mutant was reduced about 1.5-fold and 4-fold relative to that of wild-type cells when placed on TPM and CF agar, respectively (Table 3). These results show that an Δ*nla28S* mutation affects sporulation as predicted, which supports the idea that Nla28S and Nla28 are *in vivo* signal transduction partners. Why is the sporulation defect of the Δ*nla28S* mutant much weaker than that of the *nla28* mutant? One possibility is that in the Δ*nla28S* background, Nla28 is being activated (at least to some degree) by a nonspecific small molecule phosphodonor such as acetyl phosphate (Fig. 4A) or by a noncognate HK protein. Previous studies have reported nonspecific activation of RRs in the absence of their HK partners (27, 28a, 31, 43, 51); there are precedents for nonspecific activation of Nla28. It is also possible that Nla28 has more than one HK partner to modulate its *in vivo* phosphorylation state and that this partner is active in the Δ*nla28S* mutant. Thus, it seems reasonable to speculate that the developmental function of Nla28 is not completely abolished in the *nla28S* mutant, leading to a less severe development defect than that observed for the *nla28* mutant.

What might Nla28S be sensing? Nla28 begins modulating gene expression at the onset of the preaggregation stage of fruiting-body development (5). Presumably, Nla28S detects its signal during this early stage of development and activates Nla28. At this time in development, cells must closely monitor the nutrient levels in the environment to confirm that they are still starving and that embarking on a developmental process that yields dormant spores is the best course of action. Therefore, Nla28S might sense and respond to particular nutrients in the environment. Since A-signal begins to accumulate during preaggregation (20), it is also possible that Nla28S is involved in sensing and responding to this cell density signal, which is composed of a mixture of amino acids and peptides (21, 33).

Whether or not Nla28S is involved in detecting A-signal, the data presented here indicate that A-signal is important for full expression of *nla28S* and, presumably, *nla28* in developing cells (Fig. 6B). Interestingly, an *nla28* mutant fails to fully complement the developmental defect of an A-signal-deficient strain in codevelopment assays (3), suggesting that the *nla28* mutant

might be defective for A-signal production. This result is consistent with recent data showing that the promoter region of the *asgA* gene, which is important for A-signal production, contains a tandem repeat that is a good match to the Nla28 consensus binding site (Murphy et al., personal communication). Thus, it seems that A-signal and the Nla28S/Nla28 TCS may have a reciprocal relationship: expression of the genes for the Nla28S/Nla28 TCS components is modulated by A-signal, and the Nla28S/Nla28 TCS may modulate A-signal production. The goal of future work will be to explore this relationship and to examine whether nutrients, A-signal, or some other molecule is responsible for the activation of the Nla28S/Nla28 TCS during early development in *M. xanthus*.

ACKNOWLEDGMENTS

Zaara Sarwar was funded in part by an International Fellowship from the American Association of University Women (AAUW). This work was supported by National Science Foundation grant IOS-0950976 to A. G. Garza.

REFERENCES

1. **Austin S, Dixon R.** 1992. The prokaryotic enhancer binding protein NTRC has an ATPase activity which is phosphorylation and DNA dependent. EMBO J. **11**:2219–2228.
2. **Bourret RB.** 2010. Receiver domain structure and function in response regulator proteins. Curr. Opin. Microbiol. **13**:142–149.
3. **Caberoy NB, Welch RD, Jakobsen JS, Slater SC, Garza AG.** 2003. Global mutational analysis of NtrC-like activators in *Myxococcus xanthus*: identifying activator mutants defective for motility and fruiting body development. J. Bacteriol. **185**:6083–6094.
4. **Dutta R, Inouye M.** 2000. GHKL, an emergent ATPase/kinase superfamily. Trends Biochem. Sci. **25**:24–28.
5. **Giglio KM, Caberoy N, Suen G, Kaiser D, Garza AG.** 2011. A cascade of coregulating enhancer binding proteins initiates and propagates a multicellular developmental program. Proc. Natl. Acad. Sci. U. S. A. **108**:E431–E439.
6. **Goldman BS, et al.** 2006. Evolution of sensory complexity recorded in a myxobacterial genome. Proc. Natl. Acad. Sci. U. S. A. **103**:15200–15205.
7. **Gronewold TM, Kaiser D.** 2001. The act operon controls the level and time of C-signal production for Myxococcus xanthus development. Mol. Microbiol. **40**:744–756.
8. **Gronewold TMA, Kaiser D.** 2002. *act* operon control of developmental gene expression in *Myxococcus xanthus*. J. Bacteriol. **184**:1172–1179.
9. **Gronewold TMA, Kaiser D.** 2007. Mutations of the *act* promoter in *Myxococcus xanthus*. J. Bacteriol. **189**:1836–1844.
10. **Harris BZ, Kaiser D, Singer M.** 1998. The guanosine nucleotide (p)ppGpp initiates development and A-factor production in Myxococcus xanthus. Genes Dev. **12**:1022–1035.
11. **Hoch JA.** 2000. Two-component and phosphorelay signal transduction. Curr. Opin. Microbiol. **3**:165–170.
12. **Jakobsen JS, et al.** 2004. σ^{54} enhancer binding proteins and *Myxococcus xanthus* fruiting body development. J. Bacteriol. **186**:4361–4368.
13. **Julien B, Kaiser AD, Garza A.** 2000. Spatial control of cell differentiation in *Myxococcus xanthus*. Proc. Natl. Acad. Sci. U. S. A. **97**:9098–9103.

13a. **Kaiser D.** 1979. Social gliding is correlated with the presence of pili in *Myxococcus xanthus*. Proc. Natl. Acad. Sci. U. S. A. **76**:5952–5956.

13b. **Kaiser D.** 2004. Signaling in myxobacteria. Annu. Rev. Microbiol. **58**:75–98.

14. **Khorchid A, Ikura M.** 2006. Bacterial histidine kinase as signal sensor and transducer. Int. J. Biochem. Cell Biol. **38**:307–312.
15. **Kim SK, Kaiser D.** 1991. C-factor has distinct aggregation and sporulation thresholds during *Myxococcus* development. J. Bacteriol. **173**:1722–1728.
16. **Kim SK, Kaiser D.** 1990. C-factor: a cell-cell signaling protein required for fruiting body morphogenesis of M. xanthus. Cell **61**:19–26.
17. **Kroos L, Kuspa A, Kaiser D.** 1986. A global analysis of developmentally regulated genes in *Myxococcus xanthus*. Dev. Biol. **117**:252–266.
18. **Kroos L, Kaiser D.** 1987. Expression of many developmentally regulated genes in Myxococcus depends on a sequence of cell interactions. Genes Dev. **1**:840–854.
19. **Kruse T, Lobedanz S, Berthelsen NM, Søgaard-Andersen L.** 2001. C-signal: a cell surface-associated morphogen that induces and coordinates multicellular fruiting body morphogenesis and sporulation in Myxococcus xanthus. Mol. Microbiol. **40**:156–168.

19a. **Kuspa A, Kaiser D.** 1989. Genes required for developmental signalling in *Myxococcus xanthus*: three *asg* loci. J. Bacteriol. **171**:2762–2772.

20. **Kuspa A, Kroos L, Kaiser D.** 1986. Intercellular signaling is required for developmental gene expression in *Myxococcus xanthus*. Dev. Biol. **117**:267–276.
21. **Kuspa A, Plamann L, Kaiser D.** 1992. Identification of heat-stable A-factor from *Myxococcus xanthus*. J. Bacteriol. **174**:3319–3326.
22. **Kuspa A, Plamann L, Kaiser D.** 1992. A-signalling and the cell density requirement for *Myxococcus xanthus* development. J. Bacteriol. **174**:7360–7369.
23. **Lascu I, Pop RD, Porumb H, Presecan E, Proinov I.** 1983. Pig heart nucleosidediphosphate kinase. Phosphorylation and interaction with Cibacron blue 3GA. Eur. J. Biochem. **135**:497–503.
24. **Laub MT, Biondi EG, Skerker JM.** 2007. Phosphotransfer profiling: systematic mapping of two-component signal transduction pathways and phosphorelays. Methods Enzymol. **423**:531–548.
25. **Lee JS, Son B, Viswanathan P, Luethy PM, Kroos L.** 2011. Combinatorial regulation of *fmgD* by MrpC2 and FruA during *Myxococcus xanthus* development. J. Bacteriol. **193**:1681–1689.
26. **Li S, Lee BU, Shimkets LJ.** 1992. csgA expression entrains Myxococcus xanthus development. Genes Dev. **6**:401–410.
27. **Lukat GS, McCleary WR, Stock AM, Stock JB.** 1992. Phosphorylation of bacterial response regulator proteins by low molecular weight phosphodonors. Proc. Natl. Acad. Sci. U. S. A. **89**:718–722.
28. **Manoil C, Kaiser D.** 1980. Guanosine pentaphosphate and guanosine tetraphosphate accumulation and induction of *Myxococcus xanthus* fruiting body development. J. Bacteriol. **141**:305–315.

28a. **McCleary WR, Stock JB.** 1994. Acetyl phosphate and the activation of two-component response regulators. J. Biol. Chem. **269**:31567–31572.

29. **Mittal S, Kroos L.** 2009. A combination of unusual transcription factors binds cooperatively to control Myxococcus xanthus developmental gene expression. Proc. Natl. Acad. Sci. U. S. A. **106**:1965–1970.
30. **Mittal S, Kroos L.** 2009. Combinatorial regulation by a novel arrangement of FruA and MrpC2 transcription factors during *Myxococcus xanthus* development. J. Bacteriol. **191**:2753–2763.
31. **Msadek T, Kunst F, Klier A, Rapoport G.** 1991. DegS-DegU and ComP-ComA modulator-effector pairs control expression of the *Bacillus subtilis* pleiotropic regulatory gene *degQ*. J. Bacteriol. **173**:2366–2377.
32. **Parkinson JS, Kofoid EC.** 1992. Communication modules in bacterial signaling proteins. Annu. Rev. Genet. **26**:71–112.
33. **Plamann L, Kuspa A, Kaiser D.** 1992. Proteins that rescue A-signal-defective mutants of *Myxococcus xanthus*. J. Bacteriol. **174**:3311–3318.
34. **Popham DL, Szeto D, Keener J, Kustu S.** 1989. Function of a bacterial activator protein that binds to transcriptional enhancers. Science **243**:629–635.
35. **Porter SL, Armitage JP.** 2002. Phosphotransfer in *Rhodobacter sphaeroides* chemotaxis. J. Mol. Biol. **324**:35–45.
36. **Porter SC, North AK, Wedel AB, Kustu S.** 1993. Oligomerization of NTRC at the *glnA* enhancer is required for transcriptional activation. Genes Dev. **7**:2258–2273.
37. **Quon KC, Marczynski GT, Shapiro L.** 1996. Cell cycle control by an essential bacterial two-component signal transduction protein. Cell **84**:83–93.
38. **Ramakers C, Ruijter JM, Deprez RHL, Moorman AFM.** 2003. Assumption-free analysis of quantitative real-time polymerase chain reaction (PCR) data. Neurosci. Lett. **339**:62–66.
39. **Sager B, Kaiser D.** 1993. Spatial restriction of cellular differentiation. Genes Dev. **7**:1645–1653.
40. **Sasse-Dwight S, Gralla JD.** 1990. Role of eukaryotic-type functional domains found in the prokaryotic enhancer receptor factor 54. Cell **62**:945–954.
41. **Shi X, et al.** 2008. Bioinformatics and experimental analysis of proteins of two-component systems in *Myxococcus xanthus*. J. Bacteriol. **190**:613–624.
42. **Shimkets LJ.** 1990. Social and developmental biology of the myxobacteria. Microbiol. Rev. **54**:473–501.
43. **Silva JC, Haldimann A, Prahalad MK, Walsh CT, Wanner BL.** 1998. In vivo characterization of the type A and B vancomycin-resistant enterococci (VRE) VanRS two-component systems in Escherichia coli: a nonpathogenic model for studying the VRE signal transduction pathways. Proc. Natl. Acad. Sci. U. S. A. **95**:11951–11956.
44. **Singer M, Kaiser D.** 1995. Ectopic production of guanosine penta- and

tetraphosphate can initiate early developmental gene expression in Myxococcus xanthus. Genes Dev. **9**:1633–1644.
45. **Son B, Liu Y, Kroos L.** 2011. Combinatorial regulation by MrpC2 and FruA involves three sites in the *fmgE* promoter region during *Myxococcus xanthus* development. J. Bacteriol. **193**:2756–2766.
46. **Studholme DJ, Dixon R.** 2003. Domain architectures of σ^{54}-dependent transcriptional activators. J. Bacteriol. **185**:1757–1767.
47. **Ueki T, Inouye S, Inouye M.** 1996. Positive-negative KG cassettes for construction of multi-gene deletions using a single drug marker. Gene **183**:153–157.
48. **Viswanathan P, Ueki T, Inouye S, Kroos L.** 2007. Combinatorial regulation of genes essential for Myxococcus xanthus development involves a response regulator and a LysR-type regulator. Proc. Natl. Acad. Sci. U. S. A. **104**:7969–7974.
49. **Wedel A, Kustu S.** 1995. The bacterial enhancer-binding protein NTRC is a molecular machine: ATP hydrolysis is coupled to transcriptional activation. Genes Dev. **9**:2042–2052.
50. **Weiss DS, Batut J, Klose KE, Keener J, Kustu S.** 1991. The phosphorylated form of the enhancer-binding protein NTRC has an ATPase activity that is essential for activation of transcription. Cell **67**:155–167.
51. **Xu H, et al.** 2010. Role of acetyl-phosphate in activation of the Rrp2-RpoN-RpoS pathway in Borrelia burgdorferi. PLoS Pathog. **6**:e1001104. doi:10.1371/journal.ppat.1001104.